ELSEVIER

Thermochimica Acta 330 (1999) 145–154

thermochimica
acta

A combined photoacoustic DSC for simultaneous temperature modulated measurements: does it really work?

Tsvetan G. Vassilev*

Institute of Physical Chemistry, Bulgarian Academy of Sciences, 1113 Sofia, Bulgaria

Received 3 August 1998; accepted 21 January 1999

Abstract

Combination of two techniques, photoacoustic (PA) and differential scanning calorimetry (DSC), is a combination of quasi stationary thermodynamic DSC method and nonstationary dynamic PA method. Especially favorable and easy to realize is the combination with power compensated type of DSC. It has several advantages over the use of two techniques separately and allow to perform measurements simultaneously. The most obvious is simultaneous determination of thermodynamic properties such as specific heat, heat of transition and dynamic properties such as effusivity, thermal conductivity at the different phase transitions and complex specific heat at the glass transition. Unlike other temperature modulated techniques PA–DSC is especially suitable for studying polymer materials since their low thermal conductivity is an additional advantage. Conditions for simultaneous measurements are examined. It is proved that the combination of two techniques and necessary changes in construction do not essentially change adequate work of the instrument. A little disbalance of DSC operation due to the construction change can be corrected simply by recalibration. The procedures for testing and calibration for the proper operation of the combined PA–DSC are given together with some details of experimental methodology. Several measurements could serve as examples of widespread applicability of PA–DSC to study different types of phase transitions as well as time dependent processes such as glass transition. © 1999 Elsevier Science B.V. All rights reserved.

Keywords: Temperature modulated calorimetry; Photoacoustic; DSC; Phase transition; Liquid crystal; Glass transition

1. Introduction

There exists significant interest recently in literature towards the development and application of the so-called temperature modulated methods of calorimetry. This term we use for all methods which utilize temperature oscillations for studying thermal properties of matter. This interest due to the fact that these methods gives new information for phase transitions and particularly for the structural relaxation of glass forming melts. It is indicative that already commercial apparatus – temperature modulated differential scanning calorimetry (TMDSC) are in the market. In these apparatus a sinusoidal temperature modulation is added to a linear heating or cooling ramp. New information on material properties is available because of the additional information from the modulated signal. Wunderlich et al. [1] gives a thorough discussion of theory and application of TMDSC, but there also exist many different kind of homemade instruments which sometimes give better results. These include different types of AC calorimetry using Joule or light heating [2,3], 3ω method [4] and calorimetry based on photoacoustic (PA) effect [5].

---

*E-mail: vassilev@ipchp.ipc.bas.bg

PII: S0040-6031(99)00029-5

The PA effect provides a nonstationary method to investigate the change of thermal properties near the first and second order phase transitions temperature [6–9]. Buchner and Korpiun [10] have shown that the PA technique can also be used to determine the complex specific heat of the metastable liquid state near the glass transition. They have measured the frequency dependent effusivity of $CaNO_3 \cdot KNO_3$ glassforming melt instead of the specific heat itself. Kojima [9] has applied the PA method to study the thermal relaxation in "fragile" [11] liquids like propylene glycol and glycerol. Thoen [12,13] used a variable temperature PA cell coupled with magnetic field to study anisotropy in the thermal properties near phase transition of liquid crystals.

It was very useful to compare the results obtained with differential scanning calorimetry (DSC) and modulated calorimetry. For precise comparison all conditions and the sample must be identical so it is necessary to perform measurements simultaneously.

According to our knowledge, in very small number of studies so far, DSC measurements have been done to supplement [14] the AC calorimetry measurements. Recently Nishikawa and Saruyama [15] developed a light heating dynamic DSC. It measures simultaneously the DSC signal and the AC signal that goes through a sample illuminated by chopped light. They use heat flux type of DSC so the DC component must be compensated. This is done by optics which allow for the reference sample to be illuminated from the same source with the same beam power. This method uses low modulation frequencies (0.25 Hz) and the amplitude and phase shift of modulated signal is registered by temperature sensor of DSC. The limitation on the low frequency region comes from the way of detection and from the time constant of apparatus. The sample must be thermally thin compared to the thermal wavelength so that the AC signal (thermal wave) can go through sample and registered from DSC sensor.

Unlike the combined PA–DSC method previously reported [16,17] uses PA detection of the modulated signal and independent detection of the DSC signal. We use a power compensated DSC so there is no need of any compensation optics. DSC itself compensates imported DC power which result only in vertical shift of the base line. The limitation on frequencies comes from the construction of PA cell sensitivity and frequency response of microphone and the possibilities of the lock-in amplifier. Usually the frequency range for PA measurements is between several Hz and several kHz. One can work in thermally thin to thermally thick region. If one works in thermally thin regime below 0.5 Hz (which is about the usual time constant of DSC) the DSC sensor become sensitive to AC signal and only DSC detection could be used as in the described above method of Saruyama. So, two methods complement each other to enlarge the frequency range.

Such a combination provokes questions concerning the proper work of the assembly and conditions of measurements which need to be answered. First two question referring to DSC are as follows: does replacement of the standard DSC cover by PA cell change significantly the measuring condition and what is the influence of the laser beam. The proper operation of PA cell also have to be tested.

The aim of this work is to check whether the combination of two techniques DSC and PA in one is proper and is there any unfavorable influence between them which could disturb simultaneous measurements. Some experimental details and calibration procedures are also given.

2. Experimental

A chamber of a conventional DSC was adapted for variable temperature PA investigations and was described [16,17]. In this way we perform PA and DSC measurements simultaneously. Here only experimental setup and construction of the PA–DSC cell are given in Figs. 1 and 2, respectively, and explained in the captions. The DSC chamber was tightly closed by a glass cover (window) which allow the modulated (chopped) laser beam to illuminate the sample. The microphone chamber was connected to the DSC chamber by a ceramic tube. The PA signal is detected by a condenser microphone with a diameter of 1 inch. (2.54 cm). The output signal of the microphone was amplified and fed to a lock-in amplifier (PARC 5301) with built-in filter.

2.1. Testing DSC operation

For the proper operation of the power compensated type of DSC the temperature and electronic balance

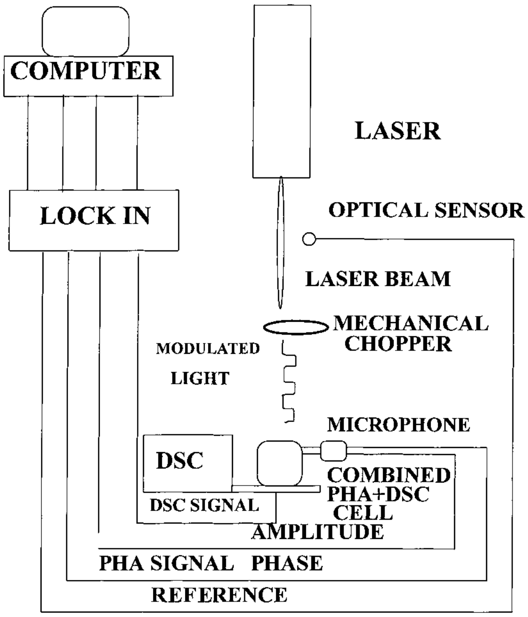

Fig. 1. Schematic diagram of the experimental setup.

between the sample oven and reference oven is very important. To be sure that changes in construction and input of additional heat source does not change dramatically these conditions, we perform the following measurements:

Two In samples of purity 99.9999 were crimped in standard Al pans in which upper surface was blackened with a thin layer of carbon black. The samples weight were 7 and 9 mg, respectively. Samples ware put in the two DSC ovens and were heated trough melting region of In with 3.125 K/min. First scan was performed with standard DCS cover, in the second scan on the place of DSC cover PA cell was mounted. The third scan was done after recalibration, with laser beam illuminating the sample. Results are shown in Fig. 3.

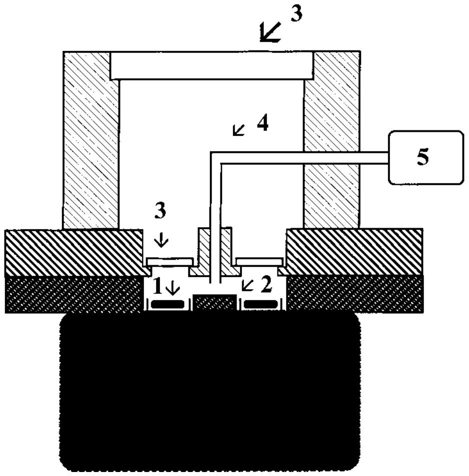

Fig. 2. Setup of the combined PA–DSC cell: (1) sample; (2) reference sample; (3) optical windows; (4) tube; (5) microphone chamber.

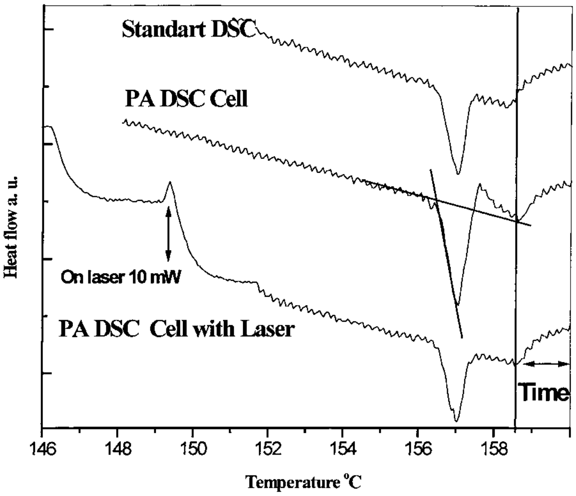

Fig. 3. DSC traces at heating 3.125 K/min of two indium samples in both ovens of DSC. Top line well calibrated standard DSC. The peak is due to difference in samples weight. Next line shows the influence of construction change. This small disbalance of the temperatures of the two ovens is easy eliminated simply by standard recalibration. Bottom line well calibrated PA–DSC instrument with illumination of laser beam of power 10 mW.

For the proper measurements with our type of DSC the temperatures of the two ovens must be identical (ΔT=Ts−Tr=0). If there was small difference in weight of samples as in our case one must observe a reduced peak in direction of sample with heavier weight (Fig. 3 top curve). In the case when there is a small difference in temperatures of the two ovens two small peaks in opposite directions are observed (Fig. 3 middle curve). Indication of that could be also a base line with large curvature. After recalibration for ΔT the second peak disappeared. Bottom curve is heat flow of well calibrated for ΔT PA–DSC cell with laser beam illumination of power 10 mW and is indistinguishable from that obtained with standard DSC cover (top line).

These two results mean that changes of the construction of DSC do not change dramatically it proper work, and the small disbalance can be corrected simply by calibration. As well that the DSC compensates completely the DC heating component of the input laser power.

It is of importance to know also whether the response of the DSC instrument to the laser beam power is linear and what is the influence of that additional heating on the sample temperature and characteristic of the transitions. This is important for both temperature and energy calibration of DSC. For this reason we studied structural phase transition of KNO_3. Powdered KNO_3 Merck sample of a purity better that 99% was pressed and placed in standard open Al pan. In order to ensure optical absorption the powder was mixed with fine particles of carbon black. The sample is heated with 3.125 K/min in the transition interval with a simultaneous laser beam illumination with power varying between 0 and 40 mW as this is illustrated in Fig. 4. The sample mass (about 50 mg) and laser power (40 mW) are up to three times larger than these we usually used in PA experiments and were selected to test the system in limiting condition. Table 1 gives temperatures of the phase transition, the energy (area), half width of the peak and its height for different laser output. The influence of the laser heating is expressed mainly by a vertical shift of the base line, while the other parameters remain unchanged within the experimental error. It is also seen that the downward drift of the base line depends linearly on power. This gives the significant advantage of the combined PA–DSC cell that it offers the possibility to evaluate the adsorbed laser beam power more precisely the efficiency with which it is converted into heat in the sample under study. The latter is important parameter for PA measurements. In principal, the technique could be used for laser absorption calorimetry. It has proven to be a useful technique to measure optical absorption of both bulk materials and thin films [18–20] which consists of measuring the resultant temperature rise of the sample, due to partial absorption of laser beam of known power. If one use acoustooptic (AOM) modulator with frequency below the time constant of DSC, experiments equivalent to the TMDSC and already mentioned method of Saruyama [15] could be performed.

Table 1

Gives the energy (area), temperature of the phase transition of KNO_3, half width of the peak and its height for different laser outputs

Laser Power (mW)	Area[a]	Peak at °C	Width °C	Height[a]
0	1	128.5	10.25	1
10	0.9986	128.4	9.75	1.0487
20	1.0132	128.4	9.75	1.0732
40	1.0253	128.3	10	1.0720

[a] The values are given with respect to the first measurement with 0 mW.

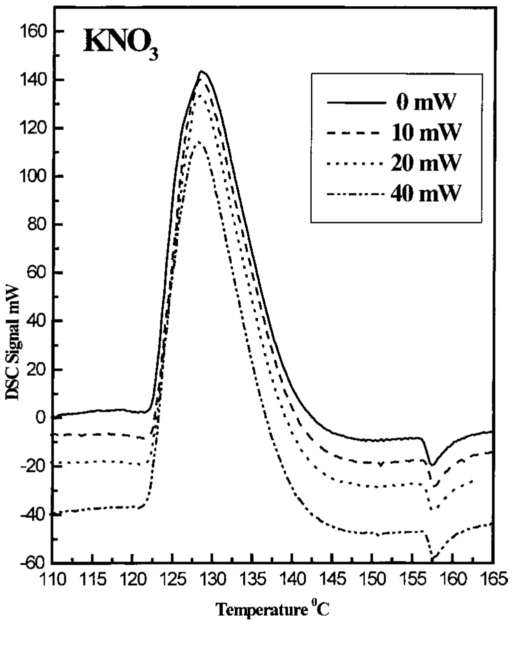

Fig. 4. DSC signal at the region of the structural phase transition of KNO_3. The sample was illuminated with different laser beam power varied from 0 to 40 mW (top to bottom).

2.2. PA signal

The PA effect has been discovered by Bell [21,22] in 1880 and was almost forgotten for a century until development of a theory which gives proper understanding of photoacoustic and photothermal effect in condensed matter [23]. After development of lasers as powerful localized energy sources the wide range of applications emerged.

In typical PA experiment the sample is placed in a tightly closed cell containing gas and illuminated by chopped light (see Figs. 1 and 2). The absorbed light is converted into heat in the sample via nonradiative deexitation processes. The absorption of periodic light produces periodic variation of sample surface temperature causing heat flow to the surrounding gas. This periodic variation generates fast decaying thermal waves which in turn cause volume and pressure fluctuations with the same frequency as the modulation frequency of the light beam in the surrounding gas. Thermal waves in the gas are reduced to less than 0.5% [23,13] at a distance of one wavelength μ ($=2\pi\mu=0.1$ cm for 100 Hz). Where μ the thermal diffusion length is equal to $\mu=(2\alpha/\omega)^{1/2}$ and $\alpha=\kappa/\rho C$ is the thermal diffusivity. This boundary gas layer responding thermally to temperature variation of sample surface can be considered as acoustic piston generating acoustic signal detected by microphone.

For the typical PA experiment one-dimensional model of Rosencwaig and Gersho's (RG) can be used. According to the RG [23] theory for the PA microphone signal $Q=qe^{-\mathrm{i}\varphi}$ with amplitude $q(T)$ and phase $\varphi(T)$ (with respect to modulation frequency) for an optically opaque and thermally thick sample PA amplitude is given by

$$q(T) = G(T)[\rho(T)k(T)C_P(T)]^{-1/2}, \tag{1}$$

and for the PA phase following Thoen [13]:

$$\tan\varphi(T) = 1 + 2[(\rho(T)C_\mathrm{p}(T))\omega/(k(T))]^{1/2}, \tag{2}$$

where T and ω are the temperature and the angular frequency, respectively, $G(T)$ accounts for the thermal properties of the cell and the coupling gas and $k(T)$, $\rho(T)$ and $C_\mathrm{P}(T)$ are the temperature dependent thermal conductivity, density and the specific heat of the sample, respectively. In principle, it is possible based on model calculation to obtain values of the product $\rho(T)k(T)C_\mathrm{P}(T)$. Since this is rather complicated one usually performs independent measurements on a sample with well known optical and thermal properties to account for $G(T)$ [24,25]. As mentioned above PA–DSC allows directly to evaluate coefficient η (efficiency with which laser beam power is converted into heat), which is important parameter for the determination of $G(T)$.

Usually the variable temperature PA cell [26–28] was build in such a way that ensures all assembly to be in thermal equilibrium including sample coupling gas to prevent convection. This impose inconvenience that very slow cooling or heating rates must be used. Unlike we use a standard possibilities of heating and cooling of DSC which are much higher. This is convenient especially when one studies sample properties that depend on thermal prehistory. In this case thermal gradients existing between the gas, sample and cell walls cause convection heat flow in the gas. These temperature gradients should be different if different scanning rates are used. It was checked for different samples (PS, PMMA, PE, In, Sn, KNO_3, alumina) that PA signal outside of transitions region do not depend on scanning rate. Since the cell size is small (below 1 cm^3) convection do not affect significantly the PA signal. The existence of convection in the gas is not so important also for absolute measurements. This is due to the fact that one have to perform calibration at every desired frequency of modulation and heating rate on the material with known thermal and optical properties to evaluate $G(T)$, as already mentioned. In this way any influences could be eliminated and scanning rates up to 10–15 K/min could be used.

2.3. PA temperature calibration

There are two sources of heat in PA–DSC cell, DSC oven and laser beam which can cause thermal gradient in the sample. For DSC measurements of polymers at heating rate of 10 K/min usually temperature gradient is up to 2 K [29] in the sample. In our measurements we usually use thin sheet polymers samples 200–300 μm and scanning rates up to 5 K/min. At this condition temperature gradient in the sample should be below 1 K. However, laser beam also cause DC heating in opposite direction. For this reason it is necessary to perform also temperature calibration of PA signal to account for the resulting thermal gradient.

Indium and liquid crystal 8OCB (4.4′-octyloxycyanobiphenyl) with commercial name M24 from Merck KgaA were used for temperature calibration of PA signal. In order to measure in thermally thick limit disk with $r=8$ mm and thickness 0.6 mm of In was used since its thermal conductivity is much higher than that of the polymers. The powder sample of 8OCB was melted to form homogeneous disk of thickness 0.3 mm. Since after melting the sample is transparent in visible spectral range a very thin alu-

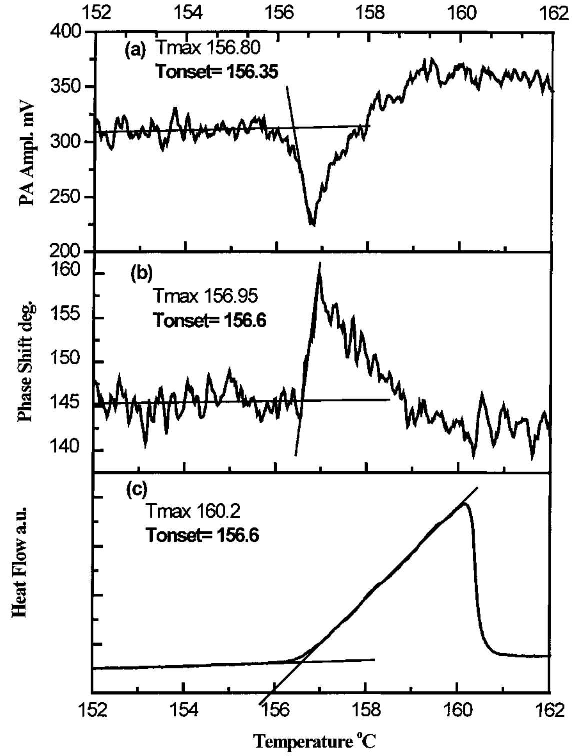

Fig. 5. Photoacoustic amplitude (a); phase shift (b); DSC signal (c) of In sample simultaneously registered at heating with 0.8 K/min and frequency 63 Hz; laser power of 34 mW. Strait lines are used for the determination of the onset. Since the sample weight is big and the DSC peak is very broad.

minum foil was placed on its upper surface. A very good and stable contact between foil and sample was obtained after first melting by slight pressing. To obtain higher signal and to reduce noise the foil was blackened.

Indium sample was heated with rate 0.8 K/min in the melting region with modulation frequency f=63 Hz and laser beam power 17 and 34 mW. Results from simultaneous PA–DSC measurements for 34 mW are shown in Fig. 5 together with temperature values of onset and maximum of the peaks. It must be noted that this value 34 mW is nominal output power of the laser and is reduced to 20 mW after going through two mirrors and two optical windows. So the effective laser beam power absorbing from the sample surface is around 60% of the output. In Fig. 6(a) and (b) PA phase shift and amplitude for 17 and 34 mW are compared. DSC curves are not given since they are indistinguishable, except for base line shift. Actually every difference between two measurements is in the range of noise. Only the mean level of the phase shift in liquid could be accepted to be different.

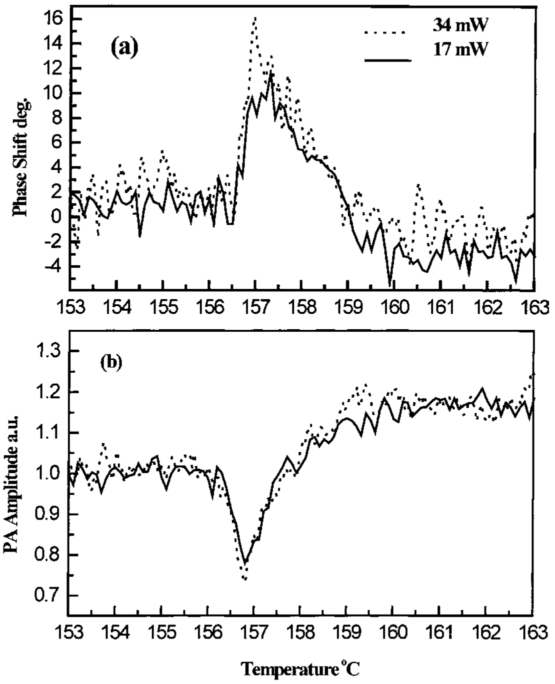

Fig. 6. Phase shift (a); photoacoustic amplitude (b) of In sample at 17 mW (solid line) and 34 mW (dotted line) laser beam power. Data are normalized in respect to the temperature below the melting point.

The values of T_{onset} and T_{max} for PA amplitude, phase shift and heat flow shows that the rule given by Korpiun and Tilgner [8] that the onset obtained from DSC must be compared with minima/maxima of the PA amplitude/phase is not very precise for combined PA–DSC measurements. Actually both values are different and higher than the DSC onset. However, the onset of PA amplitude is lower than that of DSC onset which means that the melting start from top of the sample. The anomaly of the melting in the PA signal disappears when the top surface layer of the sample with thickness equal to thermal diffusion length is molten. The onset of the phase shift is equal to the onset obtained from DSC. So for combined PA–DSC for the precise determination of the temperature the onset value of PA phase shift should be compared with onset of value obtained from DSC signal. Measurement at the same condition but with heating rate 3.125 K/min shows the same behavior. From these results is it seen that the resulting temperature gradient between top and bottom of the sample is relatively low (about 0.25 K) outside of the melting interval.

Since the heat capacity of the liquid indium is slightly greater than the solid one it looks very typical at the first glance that the level of PA amplitude is different in solid and liquid. It must be noted that the increase of PA amplitude is due to the decrease of density and thermal conductivity since PA signal is inversely proportional to the product of $k\rho$ and C_p (see Eq. (1)).

Korpiun and Tilgner (KT) [8] have developed a model for PA signal in the phase transition interval based on the suggestion of simultaneous existence of liquid and solid phases and oscillating interface between them near the melting point. After that the simultaneous existence of liquid and solid phases at the melting temperature was proven by Scanning PA Microscopy [5]. Indium melting can be well described in framework of KT model. However, it was shown in [30] that KT model in some cases give good description of anomaly of PA signal near phase transition but in other coincidence is poor or missing at all.

The 8OCB has three different phase transitions: multiple melting (327.5 K) C-S; smectic A-nematic Sa-N (340 K); nematic-isotropic N-I (353 K). The temperatures in the bracket are given according to Merck [31]. This liquid crystal is especially expedient for study. Due to proper characteristics of S-N and N-I transitions of 8OCB it was recommended [32,33] for temperature calibration on heating and cooling of standard DSC as well as TMDSC.

In Fig. 7 PA phase shift (a) amplitude (b) and DSC heat flow (c) are given for the sample of 8OCB on heating and cooling with rate 5 K/min, modulation frequency $f=16$ Hz and laser beam power of 34 mW. It is readily seen that the PA amplitude and phase shift are much more sensitive to weak S–N transition than DSC.

The regions of three phase transitions are easily distinguishable. Melting is associated with maximum in PA amplitude and step-down in PA phase shift around 50°C and depend on thermal prehistory. Next Sa-N transition is step-up in both PA amplitude and Pa phase shift at about 67°C. N-I transition at about 81°C show peak minimum and peak maximum in PA amplitude and PA phase shift, respectively. The precise temperature values of the peaks (for Sa-N transition instead of $T_{\max}$ $T_{1/2}$ are given which were determined from the half magnitude of step in PA signal) and onsets for heating of the Sa-N and of the N-I transition are given on the figure and are in good agreement with literature value given above. The difference in temperature position of Sa-N and N-I between heating and cooling is due to asymmetry between heating and cooling and thermal lag. What was said for the temperature gradient between the top and the bottom of indium sample seems to be valid also for 8OCB sample.

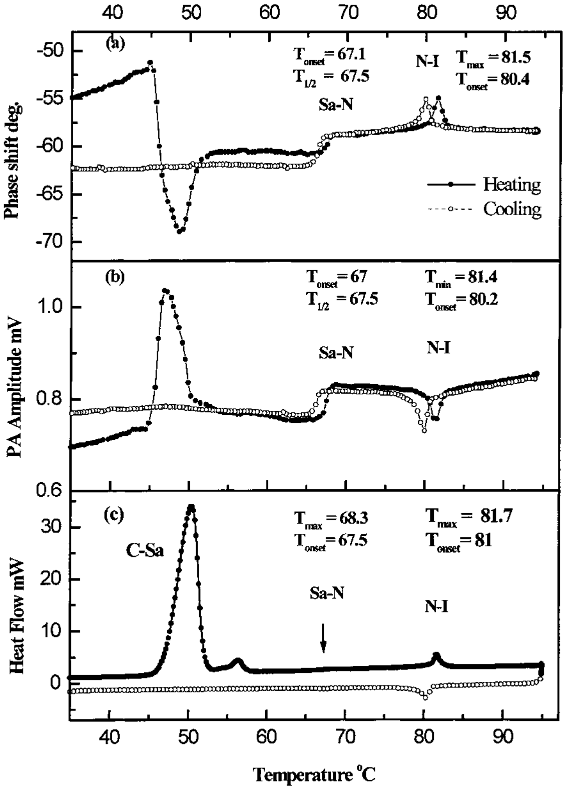

Fig. 7. Phase Shift (a); photoacoustic amplitude (b); DSC signal (c) of 8OCB liquid crystal, heating (solid circles) and cooling (open circles) with rate 5 K/min, and modulation frequency of 16 Hz, laser beam power of 34 mW.

It was found that modulation frequency have significant influence on the profile of PA amplitude an PA phase shift and could change dramatically their beha-

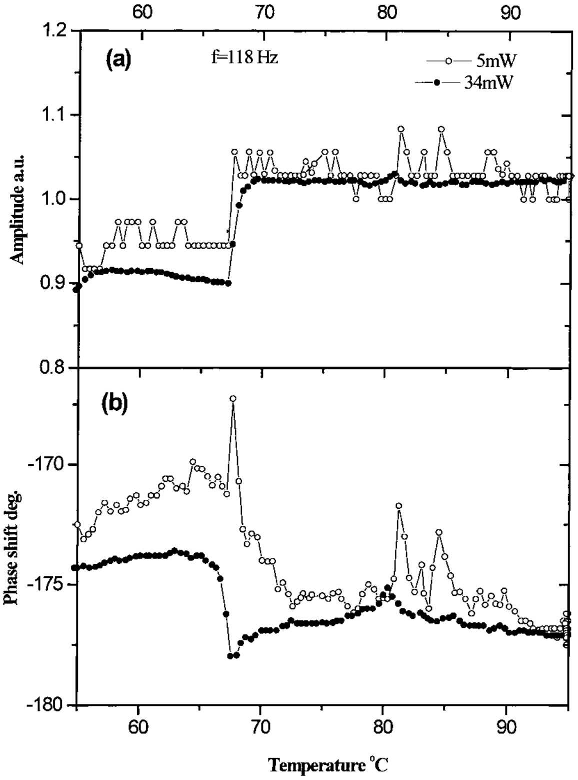

Fig. 8. Photoacoustic amplitude (a); phase shift (b) of 8OCB liquid crystal on heating with 5 K/min and modulation frequency of 118 Hz, laser beam powers of 5 mW (open circles) and 34 mW (solid circles). Data are normalized in respect to the temperature above the N-I transition.

vior at phase transition regions. However, temperature position of S-N transition remain unaffected and depend significantly only on scanning rate. This is seen from Fig. 8 where of PA amplitude an PA phase shift for two different laser beam powers 5 and 34 mW, respectively, are shown in region of S-N and N-I transitions. Measured on heating with 5 K/min and frequency 118 Hz. It is seen that the change of laser beam power by a factor of seven actually do not change the temperature position of S-N at 67.5°C. However, there are significant changes in the profile of the both PA amplitude and PA phase shift. Comparing the curves of PA phase shift from Figs. 7 and 8 it is clear that their behavior was influenced by the frequency. Phase shift at Sa-N transition changes from step-up at 17 Hz to minimum and step-down at 118 Hz. There is also the change in the behavior of the N-I transition. There are noticeable doubling in both PA amplitude PA phase shift of that transition at 5 mW. However, the magnitude of these effects is not very well reproducible. Furthermore, N-I transition move to higher temperatures as the laser beam power decrease. Comparing the curves of PA amplitude from Figs. 7 and 8 is it seen that increasing the frequency from 16 to 118 Hz change the minimum into maximum preceding of small minimum. It must be bear in mind that in PAs increasing of frequency mean also decreasing of magnitude of temperature oscillation and thermal wavelength.

Since the subject of this work is neither a nature of phase transitions in liquid crystal nor the anomaly of the PA signal near the phase transition we do not intend to discuss here this interesting behavior but rather to indicate what was experimentally observed. At present stage we do not know what is the reason for this complicated behavior of the PA signal in the interval of Sa-N and N-I transitions. We do not know also what is the reason and what information could give the fact that there is a significant difference between heating and cooling in magnitude of the step in the phase shift at Sa-N transition (see Fig. 7). One possible reason for such a dramatic change in phase shift on heating could be the change in orientational order which causes a change in thermal conductivity of 8OCB. In this case on cooling that order should not be restored until the crystallization of the sample. Thoen [13] noted the possibilities that such an anomaly near the S-N transitions could be an artifact due to high temperature gradient in the sample. However, results obtained from AC calorimetry on the same material 8OCB [34] show the same step in phase shift near S-N transition at low and high amplitude of temperature modulation. May be the thermal diffusion length is more important since this difference tend to disappear with the increase of the frequency. The role μ could be of importance because smectic phase is a layered system. In the same AC calorimetry investigation it was found doubling of N-I transition at low modulation amplitudes. These problems will be the subject of more detailed next research.

2.4. Applications

Figures shown in previous section represent also well some of the applications of PA–DSC. Results for 8OCB and In demonstrate that PA method could be

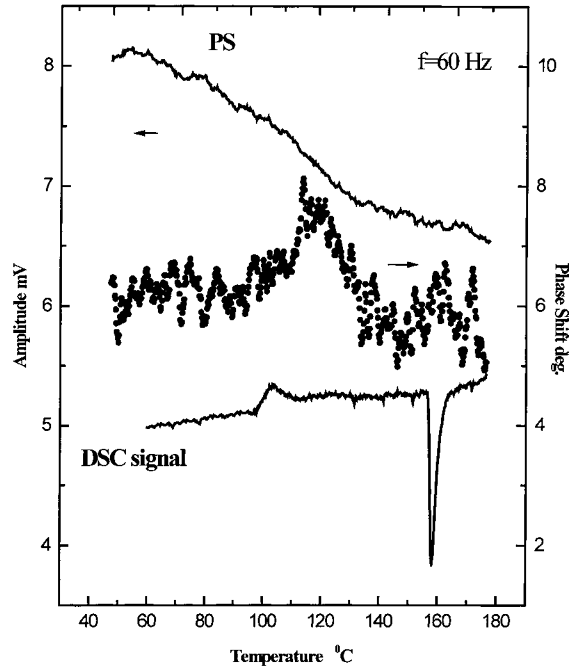

Fig. 9. Photoacoustic amplitude (solid line), phase shift (solid circles) and DSC signal (bottom line) at the glass transition interval of a-PS sample registered on heating with 3.125 K/min and modulation frequency 60 Hz.

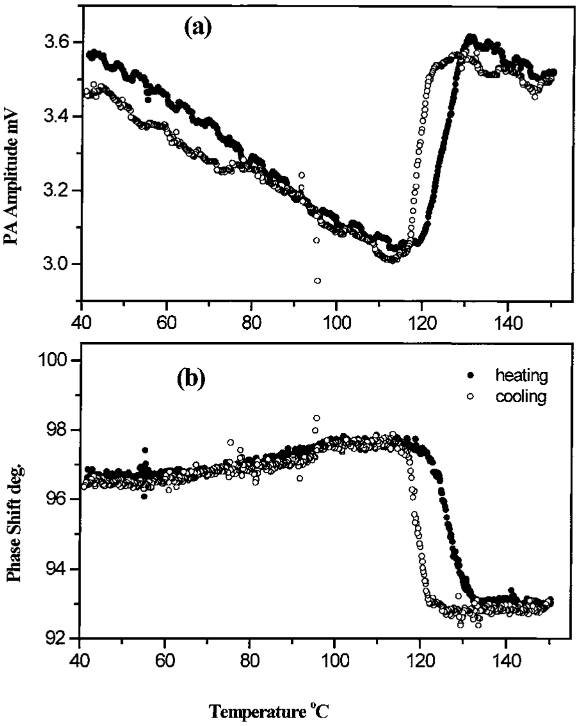

Fig. 10. PA amplitude (a); phase shift (b) of HDPE sample on heating (solid circles) and cooling (open circles) with rate 5 K/min and modulation frequency 14 Hz.

applied as a high resolution calorimetry to study different type of phase transitions.

On Fig. 9 simultaneous PA–DSC measurements at the glass transition interval of PS sample from BASF N168 are given. Two timescales of experiment are readily seen. First from underling heating rate of the DSC signal and second from modulated PA signal. After correction for $G(T)$ from PA signal one could obtain real and imaginary part of the complex C_{p}. The wide of dynamic glass transition depend of the probe frequency. Since the frequency that correspond to underling heating rate is about 10^3 less than 60 Hz the wide of the dynamic glass transition is about 40 K.

It must be noted that all results are given as row data according to the subject of the paper. No smoothing averaging or calculation are applied. Results were checked for reproducibility. In forthcoming paper we will give details about calculations needed to obtain absolute values of measured quantities.

Since from modulated PA signal and DSC one obtain the product $\rho(T)k(T)C_{\mathrm{P}}(T)$ and $C_{\mathrm{P}}(T)$, respectively, the determination $\rho T(k)(T)$ should be straightforward. Thoen [12] gives also a method for separate determination of $k(T)$ and $\rho C_{\mathrm{P}}(T)$ from PA signal. To check possibilities given by these relations will be a further step in development of PA–DSC method. Development of PA–DSC method for study of other time dependent processes such as isothermal and nonisothermal crystallization of polymer materials is in progress [35]. In Fig. 10 only as an example the anomaly in PA amplitude and phase shift at the melting and crystallization region of high density polyethylene (HDPE) are shown.

3. Conclusion

It was demonstrated that combination of PA and DSC techniques for simultaneous measurement do not lead to essential changes in their operation. Only recalibration procedure was needed when one change standard DSC cover with PA cell. In principal, the procedures proposed here for testing and calibrating should be valid for all types of power compensated DSC. All other temperature calibration concerning thermal lag should be carried out according to recommendation of GEFTA [36]. Well-developed heat flow calibration [37] procedures for conventional DSC are also directly applicable to PA–DSC.

Performing independent measurements for determining parameters and characteristics of PA cell on a sample with well known optical and thermal properties is standard in PA measurements. In this case the combined PA–DSC has an advantage directly to assess the power of absorbed light. Carbon coated alumina sample could be used for simultaneous calibration of DSC and PA signal.

Results demonstrates that PA method could be applied as a high resolution calorimetry to study different type of phase transitions and glass transition. It should be mentioned that in comparison with other TM techniques such as TMDSC, AC and PA significantly higher scanning rate could be applied in PA–DSC measurements. Some measurements show that it is possible to obtain still satisfactory results at rates as high as 15 K/min.

Acknowledgements

This work was financially supported by Program Copernicus of EU (CONTRACT IC15-CT96-0821) and Bulgarian National Science Fund (Contract X-632).

References

[1] B. Wunderlich, Y. Jin, A. Boller, Themchim. Acta 238 (1994) 277.

[2] C.W. Garland, Thermochim. Acta 88 (1985) 127.

[3] I. Hatta, Y. Sasuga, R. Kato, Maesono, Rev. Sci. Instr. 56 (1995) 1643.

[4] N.O. Birge, Phys. Rev. B 34 (1986) 1631.

[5] S. Kojima, Jpn. J. Appl. Phys. (suppl) 25(1) (1985) 215.

[6] R. Florian, J. Pelzl, M. Rosenberg, H. Vargas, R. Wernhardt, Phys. Stat. Solidi (a) 48 (1978) K35.

[7] P. Korpiun, R. Tilgner, D. Schmidt, J. de Phys. 44 (1983) C6–43.

[8] P. Korpiun, R. Tilgner, J. Appl. Phys. 51 (1980) 6115.

[9] S. Kojima, in: O.I. Leroy, M.H. Breazeale (Ed.), Physical Acoustics, Plenum Press, New York, 1991, pp. 399.

[10] B. Buchner, P. Korpiun, Appl. Phys. B 43 (1987) 29.

[11] H. Ma, X. Zhang, J. Lucas, H. Senapati, R. Bohmer, A. Angell, J. Solid State Chem. 96 (1992) 181.

[12] J. Thoen, Handbook of Liquid Crystals, vol. 1, Chapter on: Thermal Methods, 1997, p. 30.

[13] J. Thoen, C. Glorieux, Thermochim. Acta 304/305 (1997) 137.

[14] S. Weyer, A. Hensel, J. Korusb, E. Donth, C. Schick, Thermchim. Acta 304/305 (1997) 251.

[15] M. Nishikawa, Y. Saruyama, Thermochim. Acta 267 (1995) 75.

[16] T. Vassilev, T. Velinov, I. Avramov, S. Surnev, Appl. Phys. A 61 (1995) 129.

[17] T. Vassilev, T. Velinov, I. Avramov, S. Surnev et al., Solid State Commun. 91 (1994) 49.

[18] A. Hordvik, Appl. Opt. 16 (1977) 2827.

[19] L. Skolnik, in: S.S. Mitra, B. Bendow (Eds.), Optical Properties of Highly Transperent Solids, Plenum Press, New York, 1975, pp. 405.

[20] D.J. Gallant, Rev. Sci. Instr. 59 (1988) 2241.

[21] A.G. Bell, Am. J. Sci. 20 (1880) 305.

[22] A.G. Bell, Philos. Mag. 5(11) (1881) 510.

[23] A. Rosencwaig, A. Gersho, J. Appl. Phys. 47 (1976) 64.

[24] J. Thoen, C. Glorieux, E. Schoubs, W. lauriks, Mol. Cryst. Liq. Cryst. 191 (1990) 29.

[25] C. Glorieux, E. Schoubs, J. Thoen, Mat. Sci. Eng. A 122 (1989) 87.

[26] C. Pichon, M. de Liboux, D. Fournier, A.C. Boccara, Appl. Phys. Lett. 35 (1979) 435.

[27] P.S. Bechtold, M. Campagna, Optics Commun. 36 (1981) 373.

[28] P.S. Bechtold, J. Photoacoustics 1 (1982) 82.

[29] J. Schawe, C. Schick, Thermchim. Acta 187 (1991) 335.

[30] T. Somasundaram, P. Ganguly, C.N. Rao, J. Phys. C 19 (1986) 2137.

[31] Merck KgaA, Darmstadt, Germany.

[32] G.W.H. Höhne, J. Schawe, C. Schick, Thermochim. Acta 221 (1993) 129.

[33] A. Hensel, C. Schick, Thermchim. Acta. 304/305 (1997) 229.

[34] A. Minakov, C. Schick, AC calorimetery of polymers in glass and melting transitions, 317 (1998) 117.

[35] T. Vassilev et al., in preparation.

[36] M. Sarge, W. Hemminger, E. Gmelin, G.W.H. Höhne, H.K. Cammenga, W. Eysel, J. Thermal Anal. 49 (1997) 1125.

[37] G.W.H. Höhne, H.K. Cammenga, W. Eysel, E. Gmelin, W. Hemminger, Thermochim. Acta 160 (1990) 1.